Published in final edited form as:
Cancer Res. 2008 September 15; 68(18): 7313–7322. doi:10.1158/0008-5472.CAN-08-0598.

Interaction of *Muc2* and *Apc* on Wnt signaling and in intestinal tumorigenesis: potential role of chronic inflammation

Kan Yang[1,a], **Natalia V. Popova**[2,a], **WanCai Yang**[3], **Ioanna Lozonschi**[2], **Selam Tadesse**[2], **Scott Kent**[2], **Laura Bancroft**[2], **Ilze Matise**[4], **Robert T. Cormier**[5], **Stefan J. Scherer**[6], **Winfried Edelmann**[6], **Martin Lipkin**[1], **Leonard Augenlicht**[2,6], and **Anna Velcich**[2,b]

1 *Strang Cancer Center at New York Blood Bank, New York, NY*

2 *Department of Oncology, Albert Einstein Cancer Center/Montefiore Medical Center, Bronx, NY*

3 *Department of Pathology, University of Illinois at Chicago, Chicago, IL*

4 *University of Minnesota, College of Veterinary Medicine, St. Paul, MN*

5 *University of Minnesota Medical School, Duluth, MN*

6 *Department of Cell Biology, Albert Einstein College of Medicine, Bronx, NY*

Abstract

Somatic mutations of the Adenomatous polyposis coli (*APC*) gene are initiating events in the majority of sporadic colon cancers. A common characteristic of such tumors is reduction in the number of goblet cells that produce the mucin MUC2, the principal component of intestinal mucus. Consistent with these observations, we demonstrated that Muc2 deficiency results in the spontaneous development of tumors along the entire gastrointestinal tract, independently of deregulated Wnt signaling. To dissect the complex interaction between Muc2 and Apc in intestinal tumorigenesis, and to elucidate the mechanisms of tumor formation in *Muc2*$^{-/-}$ mice, we crossed the *Muc2*$^{-/-}$ mouse with 2 mouse models, *Apc*$^{1638N/+}$ and *Apc*$^{Min/+}$, each of which carries an inactivated *Apc* allele. The introduction of mutant *Muc2* into *Apc*$^{1638N/+}$ and *Apc*$^{Min/+}$ mice greatly increased transformation induced by the *Apc* mutation and significantly shifted tumor development towards the colon, as a function of *Muc2* gene dosage. Furthermore, we demonstrated that in compound double mutant mice deregulation of Wnt signaling was the dominant mechanism of tumor formation. The increased tumor burden in the distal colon of *Muc2/Apc* double mutant mice was similar to the phenotype observed in *Apc*$^{Min/+}$mice that are challenged to mount an inflammatory response, and consistent with this, gene expression profiles of epithelial cells from flat mucosa of Muc2 deficient mice suggested that Muc2 deficiency was associated with low levels of subclinical chronic inflammation. We hypothesize that Muc2$^{-/-}$ tumors develop through an inflammation related pathway that is distinct from, and can complement, mechanisms of tumorigenesis in *Apc*$^{+/-}$ mice.

Introduction

Muc2 expressed by goblet cells is the most abundant secreted intestinal mucin, the protein component of the viscous-elastic mucus that protects the intestinal epithelium against mechanical and chemical insults (1). Altered MUC2 expression and/or glycosylation accompany intestinal pathologies, including Inflammatory Bowel Disease and colon cancer (2). The importance of MUC2 in intestinal homeostasis is reflected by alterations of cell

bCorrespondence E-mail: velcich@aecom.yu.edu.
[a]These authors contributed equally to this work.

proliferation, migration and apoptosis in the mouse intestine upon genetic inactivation of the *Muc2* gene (3). Increased proliferation and survival of the epithelial cells in *Muc2*$^{-/-}$ mice may be a direct consequence of increased exposure of the cells to the luminal contents, and may be an environment for tumor initiation and promotion. Indeed, *Muc2* deficient mice develop small and large intestinal, and rectal, tumors (3). Therefore, loss of Muc2 can be an initiating event in intestinal tumorigenesis.

Intestinal tumorigenesis is most frequently initiated by mutations in *APC*, a component of the Wnt/β-catenin signaling pathway. APC mutations characterize tumors in Familial Adenomatous Polyposis (FAP), an inherited form of colon cancer, and also 80% of sporadic colon cancers (4–6), affecting the activity of β-catenin/TCF4, resulting in altered intestinal homeostasis characterized by activation and repression of genes that regulate the orderly process of cell maturation along the crypt-lumen axis, leading to tumor development (7).

Consistent with observations that lack of Muc2 can be an independent initiating event, we showed that tumors from *Muc2*$^{-/-}$ mice do not have alterations of Wnt/β-catenin/Tcf4 signaling (3). There is, however, evidence of interaction between APC and MUC2 in the early steps of tumorigenesis. For example, in tumors initiated by mutant APC there is under representation of goblet cells, the cell lineage that expresses MUC2, consistent with repression of *HATH1* and *CDX2*, two positive regulators of MUC2 expression (8,9), by activated Wnt signaling. Similarly, depletion of goblet cells, and mucin reduction, occurs in a subset of Aberrant Crypt Foci (ACF) (10), pre-neoplastic lesions in intestinal tumor development (11). Therefore, to dissect complex interactions between MUC2 deficiency and *APC* mutation, and to elucidate mechanisms of tumor formation in *Muc2*$^{-/-}$ mice, we crossed the *Muc2*$^{-/-}$ mouse with 2 mouse models of *Apc* initiated intestinal cancer: *Apc*$^{1638N/+}$ (12) and *Apc*$^{Min/+}$ (13). We report that introduction of the mutant *Muc2* allele into these strains greatly exacerbated mutant *Apc* initiated transformation as a function of mutant *Muc2* gene dosage, and shifted tumor incidence towards the colon, a phenotype similar to that of *Apc*$^{Min/+}$ mice challenged to mount an inflammatory response (14,15). Moreover, intestinal epithelial cells of the flat mucosa of *Muc2*$^{-/-}$ mice were characterized by a gene expression profile consistent with subclinical levels of chronic inflammation. Thus, we hypothesize that Muc2 deficiency establishes an inflammatory stimulus that modulates mutant *Apc* initiated transformation, and that Muc2$^{-/-}$ tumors develop through an inflammation related pathway distinct from, but interactive with, pathways recruited in tumor formation in *Apc*$^{+/-}$ mice.

Materials and Methods

Mice

Muc2/Apc$^{1638N/+}$ mice were on the B6/129/Ola mixed background; compound double mutant *Muc2/Apc*$^{Min/+}$ mice were on a congenic C57BL/6 background. Details of procedures are provided in Supplementary Data.

Western blot analysis

Cell extracts from intestinal polyps and flat mucosa were prepared by sonicating pulverized tissue in sample buffer. Intestinal epithelial cells (IEC) were isolated from 3 month old mice (3 mice/genotype; Supplementary Data).

DNA and RNA isolation

Genomic DNA was isolated from frozen tissue using the DNeasy tissue kit (Qiagen). Total RNA was isolated from frozen, pulverized tissue, or purified intestinal epithelial cells, using Trizol (Invitrogen), treated with RQ1 RNAse free DNAseI (Promega) for 15 min at room temperature.

Microarray analysis

Total RNA was purified from intestinal epithelial cells from the duodenum of age/gender matched *Muc2*$^{-/-}$ and wt mice, three mice per genotype, at 3 and 6 months of age, and processed using Affimetrix protocols and Affymetrix mouse 430 arrays (Supplementary Data).

Quantitative RT-PCR

Total RNA was isolated from purified intestinal epithelial cells from duodenum of each of 3 *Muc2*$^{-/-}$ and 3 wt 3 month old, gender matched mice. RNA was reverse transcribed into cDNA (SuperScriptIII reverse transcriptase, Invitrogen). Amplification employed a 7900HT ABI machine (Applied Biosystems) using SYBER Green Core reagent kit. Samples were analyzed in duplicate; quantification of relative gene expression level used the standard curve method (User Bulletin #2, ABI), with values normalized to β-actin or ribosomal protein L41 (Rpl41). Primer sequences are in Supplementary Table 1.

In vitro transcription and translation assay (IVTT)

Amplification of DNA with primers specific for the wt *Apc* allele produced segment 1, spanning nucleotide 1991–5142 in exon 15 of the *Apc* gene (Acc.# M88127). This was used to generate 2 overlapping fragments (segment 2, codons 677–1234; segment 3, codons 1100–1690), which were used to program the IVTT system (TNT T7 Quick coupled transcription/translation System, Promega). Products were analyzed by SDS-PAGE and fluorography (16), and mutant clones characterized by sequencing. Primer sequences are in Supplementary Table 1.

Loss of heterozygosity and microsatellite instability (MSI) analysis

Ten ng of genomic DNA from tumors and normal tissue, and serial dilutions (1:2 and 1:4) were tested in triplicate by genomic qPCR amplification of the wt and the mutant *Apc* allele in separate reactions. In each run DNA from *Apc*$^{1638N/+}$ mouse liver was assessed to monitor consistency. Relative quantification of wt and mutant *Apc* allele was determined using the standard curve method (above). The ratio between mutant and wt *Apc* allele was determined for normal and tumor samples; LOH was defined by a mut/wt value above the maximum value from the compilation of normal tissue samples, as described (15).

MSI was analyzed by amplifying 50 ng of genomic DNA from paired normal and tumor samples using ^{32}P end-labeled primers, with PCR products analyzed by electrophoresis on denaturing 6% polyacrylamide gels and bands visualized using the Storm Imaging System or autoradiographic films. Analysis was of 5 di-nucleotide repeats (*D7Mit91*, *D17Mit123*, *D1Mit36*, *D15Mit93*, *D10Mit2*) and 2 mono-nucleotide repeats (*U12235*, and a T24 tract in *uPAR* (17)).

Immunohistochemistry

5μm sections from formalin fixed, paraffin embedded samples were analyzed (Supplementary Data). The list of antibodies is in Supplementary Data.

Results

The inactivated *Muc2* allele exacerbates the tumor phenotype of the *Apc*$^{1638N/+}$ mouse by a gene dosage dependent mechanism

Since tumors in *Muc2*$^{-/-}$ mice develop through a Wnt independent pathway, we crossed *Muc2*$^{-/-}$ with *Apc*$^{1638N/+}$ mice, a model of intestinal cancer caused by a mutant *Apc* allele. Introduction of the *Muc2* mutation, both in the heterozygous and homozygous state, accelerated tumor development, increasing both tumor incidence and multiplicity (Suppl. Fig. 1; Table 1A). Tumors increased at three months and progressed with age. At 12 months, heterozygosity and nullizygosity for *Muc2* caused almost a doubling and >3 fold increase, respectively, in tumor multiplicity. *Muc2*$^{+/-}$ mice lack a detectable phenotype (3). Here, only one of 11 52 week old *Muc2*$^{+/-}$ mouse had a single small intestinal tumor (Table 1A). In contrast none of the wt mice developed gastrointestinal tumors (not shown). Thus, Muc2 heterozygosity imparted a very low risk of tumors that was enhanced when combined with a stress stimulus, the *Apc*$^{1638N/+}$ background. That *Muc2* and *Apc* mutations were at least additive for tumor development in a compound mutant mouse is a further indication that mutations at these loci operate through distinct mechanisms. In addition, the distribution of tumors was substantially altered; double mutant mice developed tumors along the entire colon, though there were more tumors in the left colon than in the right. An example of tumor histology is shown in Suppl. Fig 2.

While *Apc*$^{1638N/+}$ mice have a low penetrance tumor phenotype in the colon (3 distal colonic tumors in 44 mice studied), ~ 70% of *Apc*$^{Min/+}$ mouse develop ~2 tumors/mouse in the distal colon and rectum by 120 days. Therefore, we also crossed the *Muc2*$^{-/-}$ mouse with the *Apc*$^{Min/+}$mouse. Due to early mortality, sacrifice was at 75 days of age. The phenotype of double mutant *Muc2*$^{-/-}$; *Apc*$^{Min/+}$mice was qualitatively similar to that of *Muc2*$^{-/-}$;*Apc*$^{1638N/+}$ mice, although remarkably more severe (Table 1B). There was a carpet of tumors in the distal colon of all compound mutant mice (Suppl. Fig. 3), with only a few tumors in the proximal colon, and a significant increase in tumor number in the small intestine of *Muc2*$^{-/-}$;*Apc*$^{Min/+}$mice. For *Muc2*$^{+/-}$;*Apc*$^{Min/+}$ mice, survival was longer and mice were sacrificed at either 75 or 120 days of age. Similar to *Muc2*$^{+/-}$; *Apc*$^{1638N/+}$ mice, the *Apc*$^{Min/+}$ phenotype was affected by *Muc2* haploinsufficiency, reflected in a less prominent, yet significant, increase of colonic tumors at 75 (Table 1B) and 120 days (data not shown). In the small intestine, tumor burden increased at 75 days (Table 1B) and became more pronounced in older mice (not shown). Thus, introduction of the *Muc2* mutation modulated the tumor phenotype of mouse models carrying a mutant *Apc* allele, irrespective of the nature of the *Apc* mutation, and the extent of this modulation was *Muc2* gene dosage dependent.

In *Muc2*$^{-/-}$ mice 50% of colonic tumors were carcinomas, but in *Muc2*$^{-/-}$; *Apc*$^{1638N/+}$ mice only 17% (17/102) were carcinomas, and 83% adenomas. All *Muc2*$^{+/-}$*; Apc*$^{1638N/+}$ colonic tumors were adenomas. In *Muc2*$^{-/-}$;*Apc*$^{Min/+}$ colonic tumors, there was a continuum of proliferative lesions that included hyperplasia, dysplasia and adenoma. Thus, though the colon of double mutant mice developed many more tumors, they rarely presented as carcinomas, possibly due to increased mortality of double mutant mice from tumor burden, also indicated by the shorter life span of *Muc2*$^{-/-}$; *Apc*$^{Min/+}$mice, thus precluding progression to carcinoma as a function of time.

Characterization of tumors of *Muc2*$^{-/-}$, *Apc*$^{1638N/+}$ mice, and compound double mutant mice

We first determined whether tumors from compound double mutant mice exhibited altered Wnt signaling, as in *Apc*$^{1638N/+}$ tumors, or lacked deregulated Wnt, as in *Muc2*$^{-/-}$ tumors. Tumors from *Muc2*$^{+/-}$;*Apc*$^{1638N/+}$ and *Muc2*$^{-/-}$;*Apc*$^{1638N/+}$ mice exhibited increased accumulation of β-catenin in the cytoplasm and in the nucleus (Fig 1A), suggesting that these tumors had an altered Apc pathway. This was confirmed by elevated levels of active (dephosphorylated) β-catenin in tumors of compound mutant mice compared to adjacent normal mucosa, similar to overexpression of active β-catenin in *Apc*$^{1638N/+}$ tumors. In contrast, there was little difference in levels of active β-catenin in Muc2$^{-/-}$ tumors and adjacent normal mucosa (Fig. 1B). Quantitative data of active β-catenin relative to total β-catenin in tumors and adjacent normal tissue in *Muc2*$^{-/-}$ and *Muc2*$^{-/-}$;*Apc*$^{1638N/+}$mice are shown in Suppl. Fig. 4.

The fundamental role of cyclo-oxygenase 2 (Cox2) in intestinal tumorigenesis in the context of deregulated Wnt signaling is well established (18). Western blot analysis of paired tumor-normal samples showed robust elevation of Cox2 levels in tumors of *Muc2*$^{-/-}$, *Muc2*$^{+/-}$;*Apc*$^{1638N/+}$, *Muc2*$^{-/-}$ *;Apc*$^{1638N/+}$, and *Apc*$^{1638N/+}$ mice (Fig. 1B). Immunohistochemical analysis confirmed that, as previously shown in the *Apc*$^{Min/+}$ and *IL10*$^{-/-}$ mice (19,20), Cox2 positivity was detected in tumor infiltrating stromal cells, but not in the flat mucosa of the *Muc2*$^{-/-}$, *Apc*$^{1638N/+}$ mice (Supplementary Fig. 5). Thus, elevation of Cox2 expression in intestinal tumors is a common feature of these genotypes, and is not linked to the etiology and earliest event of tumor initiation, but may represent convergence on a common mechanism.

Muc2 gene dosage is linked to the molecular mechanisms of inactivation of the wt *Apc* allele

In tumors from *Apc*$^{1638N/+}$ mice, the wt *Apc* allele is lost in the great majority of cases, or, less frequently, inactivated by somatic mutations that produce a truncated Apc protein unable to drive β-catenin degradation, resulting in β-catenin accumulation, and nuclear translocation. Similarly, we observed nuclear accumulation of β-catenin in tumors from *Apc*$^{1638N/+}$ mice that were either heterozygous or homozygous for mutant *Muc2* mutant (Fig. 1A). We therefore ascertained the status of the wt *Apc* allele by *in vitro* transcription-translation (IVTT), interrogating *Apc* exon 15 spanning codons 664–1690, the region homologous to the mutation cluster region (MCR) of human APC, which preferentially accumulates such mutations (16). In this assay, a chain terminating mutation yields a peptide smaller than that encoded by the wild-type allele. Representative examples of size fractionated IVTT generated polypeptides are shown in Supplementary Fig. 6, with results summarized in Table 2. None of the 30 Muc2$^{-/-}$ tumors harbored mutant Apc polypeptides (Suppl. Fig. 6A), confirming that mutated Apc was not present in Muc2$^{-/-}$ tumors, and consistent with the lack of nuclear β-catenin accumulation (above, and (3). However, 50% of the tumors (12/24 table 2) from *Muc2*$^{+/-}$;*Apc*$^{1638N/+}$ mice had truncating *Apc* mutations, as shown by shorter peptides (Suppl. Fig. 6A,B, T7–12). All but 1 mutation were in segment 2 (T12 in Suppl. Fig. 6B). Surprisingly, less than 15% of *Muc2*$^{-/-}$; *Apc*$^{1638N/+}$ tumors had truncating *Apc* mutations (Table 2). This difference in frequency of truncating mutations in tumors between *Muc2*$^{+/-}$;*Apc*$^{1638N/+}$ and *Muc2*$^{-/-}$; *Apc*$^{1638N/+}$mice was significant ($P \leq 0.01$, 2 sided χ^2 test).

All PCR products that generated mutant peptides in the IVTT assay were cloned and sequenced; data are summarized in Table 2 and Supplementary Table 2. The majority of *Apc* mutations in the Muc2$^{+/-}$; Apc$^{1638N/+}$ tumors were base substitutions (8/12), with 6 of these transitions (6/12). Interestingly, of these 6 transitions, 4 were C to T transitions, and half occurred at CpG islands coding for Arg^{854}, a mutational hot spot in compound MMR deficient/*Apc*$^{1638N/+}$ mice (16), Supplementary Table 2). The remaining 2 base substitutions were G to T mutations at codon 866. The remaining 4 tumors from *Muc2*$^{+/-}$;*Apc*$^{1638N/+}$ mice with mutated *Apc* alleles harbored frame shift mutations due to insertions/deletions of a single nucleotide in mononucleotide repeats. In contrast, all *Apc* truncating mutations of the 4 *Muc2*$^{-/-}$; *Apc*$^{1638N/+}$ tumors were base substitutions, 2 of which were C to T transitions and 2 G to T transversions (Supplementary Table 2). Thus, not only were there fewer *Apc* mutations in tumors from the *Muc2*$^{-/-}$; *Apc*$^{1638N/+}$ mice compared to tumors from the *Muc2*$^{+/-}$;*Apc*$^{1638N/+}$ mice, but the mutation spectrum differed between these genotypes.

The spectrum of mutations in the *Muc2*$^{+/-}$;*Apc*$^{1638N/+}$ tumors was reminiscent of that in tumors of compound double mutant MMR deficient/*Apc*$^{1638N/+}$ mice (16). We, therefore, analyzed paired normal/tumor DNA from mice of the three different genotypes for the presence of microsatellite instability (MSI), diagnostic for MMR defects, using 7 different markers (Methods) None of the tumors analyzed, including those characterized by the presence of truncating mutation in the wt *Apc* allele, displayed MSI (an example is shown in Suppl. Fig. 7). These data suggest that tumors from *Muc2*$^{-/-}$ and compound double mutant *Muc2; Apc*$^{1638N/+}$ mice were not MSI, a form of genetic instability that can have a causative role in tumor development, despite the fact that heterozygous inactivation of *Muc2* increases mutation frequency of the wt *Apc* allele in the compound mutant mice.

Loss of heterozygosity (LOH) is the most frequent mechanism of inactivation of the wt *Apc* allele in tumors of $Apc^{1638N/+}$ mice (21). Thus, we investigated whether tumors that did not show truncating mutation of *Apc* were instead characterized by LOH. We determined, by qPCR, the ratio between mutant and wt *Apc* alleles using primers that amplify only the mutant or the wild type *Apc* allele in DNA from paired tumor and normal tissues, as well as from normal spleen, liver, and tails. Data were analyzed as described (15). Control DNAs from normal tissue displayed a median value of the ratio between mutant and wt allele of 1.12 and a maximal value of 1.35. Thus, a ratio of mut/wt *Apc* allele greater than 1.35, was considered positive for LOH. Among tumors that had mutational inactivation of the wt *Apc* allele we generally did not detect LOH (Fig 2), with only 5 of 16 tumors showing LOH (31%, Table 3). However, LOH was not significantly enriched in the tumors that were not characterized by mutation in the wt *Apc* allele. Of 26 tumors analyzed that did not exhibit detectable *Apc* mutation, only 10 displayed LOH (38%). As controls, 83% (5/6) of tumors from $Apc^{1638N/+}$ mice exhibited LOH, in agreement with published data (21). Interestingly, when we analyzed the data as a function of *Muc2* mutation, we found that the majority of tumors (65%) from $Muc2^{+/-}$; $Apc^{1638N/+}$ mice either had mutation or LOH of wt *Apc*. However, in tumors from $Muc2^{-/-}$; $Apc^{1638N/+}$ mice, only 36% (8/22) of tumors had either mutation or LOH of wt *Apc*, despite the fact that our molecular analyses demonstrated that tumors in compound double mutant mice develop through deregulation of Wnt signaling (Fig. 1A and B and suppl. Fig 4).

Epithelial cells of $Muc2^{-/-}$ flat mucosa display a transcriptional signature reflecting inflammation

The colonic tumor phenotype of compound double mutant *Muc2/Apc* mice is reminiscent of $Apc^{Min/+}$mice treated with dextran sodium sulfate (DSS) (14), R. Cormier, unpublished), a model of intestinal inflammation, and in compound $Smad3^{-/-}$;$Apc^{Min/+}$mice in which inactivation of *Smad3* triggers inflammation (15). This suggested that lack of Muc2 might provide an inflammatory stimulus. Therefore, to investigate whether absence of Muc2 causes low level, chronic, subclinical inflammation that alters intestinal homeostasis we compared gene expression profiles of epithelial cells isolated from the duodenum of wild-type (wt) mice or $Muc2^{-/-}$ mice, at 3 and 6 month of age. At 3 months, of 41,530 sequences assayed, the expression pattern of 951 (~ 2%), corresponding to 669 distinct genes, were altered significantly in $Muc2^{-/-}$ compared to wt mice, with more genes repressed (525) than induced (144) in the $Muc2^{-/-}$ flat mucosa (partial list in Supplementary Table 3). The most highly downregulated genes included members of the families of phase I and II detoxifying enzymes involved in xenobiotic metabolism, including cytochrome P450, (Cyp) family (*Cyp1a1*, *Cyp2a10*, *-3a11* and *-4a10*), greatly downregulated in the small intestine of both 3 and 6 month old $Muc2^{-/-}$ mice, as well as glutathioneS-transferases (*Gst*), UDP-glucoronosyl transferases (*UDP-Gt*), sulfotransferase; and *Nqo1*. Although these enzyme complexes are generally induced as a component of an adaptive defense response to environmental stress, they can be repressed in chronic inflammation (reviewed in (22)). In addition, genes of the antioxidant response were downregulated, such as catalase and *Glrx1*, with the notable exception of glutathione reductase (*Gsr*) and glutathione peroxidase2 (*Gpx2*) that are involved in inactivation of hydroperoxides and regeneration of GSH; however, *Gclm*, the modifier subunit of glutamate-cysteine ligase, the rate limiting enzyme in synthesis of GSH, was significantly downregulated. The repression of several of these genes was confirmed by q-RT PCR (Fig. 3A).

Interestingly, and consistent with these data in the $Muc2^{-/-}$ mice, it was recently shown (23) that in a rat model of IBD, there was a robust inhibition of several Cyp members, with evidence that endotoxins of commensal bacteria contribute to these effects. In this regard, a role of commensal bacteria in developing a reactive intestinal mucosa in *Muc2*$^{-/-}$ mice can be inferred from elevation of several genes expressed by Paneth cells that have anti-bacterial activity, including angiogenin4 (*Ang4*), matrylisin (*Mmp7*), secretory phospholipase A2 (*Pla2g2a*, and *Pla2g5*), and *RegIIIγ* (Fig. 3B), the latter recently shown to have specific bactericidal activity against Gram-positive bacteria (24). Moreover, levels of RegIIIγ are decreased in mice deficient for *Retnlb/Relmβ*, a member of the resistin family specifically expressed in intestinal goblet cells, implying positive regulation of *RegIIIγ* by Retnlb (25). Accordingly, we detected increased levels of *Retnlb*, in *Muc2*$^{-/-}$ mice (Fig 3B). The importance of Relmβ in intestinal inflammation is underscored by demonstration that its inactivation protects mice from DSS induced colitis (25). Additional members of the C-type lectin family expressed in Paneth cells were induced such as *Pap1* and *Mbl2* (Fig. 3B). Further, lipocalin2 (*Lcn2*), which regulates bacterial growth by iron sequestration (26), was greatly upregulated in Muc2$^{-/-}$ mucosa. Consistent with upregulation of genes of the innate immune response, we detected elevated expression of two members of the CC chemokine family (*Ccl6* and *Ccl28*) expressed by intestinal epithelial cells to promote antimicrobial immunity (27,28), as well as *Ifn-γ*.

Importantly, some of these changes in the duodenum were also detected in epithelial cells of *Muc2*$^{-/-}$ colonic flat mucosa. We found that 30% of the gene expression changes associated with the Muc2$^{-/-}$ duodenum (14 of the 46 genes listed in Suppl. Table 3) overlap with similar changes in the colon of *Muc2*$^{-/-}$ mice. Of these, *Ang4* and *Reg1* changed in opposite direction. Additionally 2 genes, *Intelectin a* and *Defensin5*, that showed no changes in the duodenum of *Muc2*$^{-/-}$ mice, were greatly downregulated in the colon of *Muc2*$^{-/-}$ mice. Interestingly, both genes are normally expressed in the small intestine providing defense against microbes. The partial overlap of the changes that we detected in duodenum and colon of *Muc2*$^{-/-}$ mice most likely reflects distinct patterns of gene expression that characterizes these different segments of the normal intestinal tract.

Therefore, despite the absence of significant infiltration of inflammatory cells and of obvious inflammation-related histopathology under the conditions used in this study, these data suggest that the mucosa of *Muc2*$^{-/-}$ mice reflects an inflammatory response to low levels of inflammation.

To better characterize inflammation in *Muc2*$^{-/-}$ mice we determined the basal level of expression of chemokines/cytokines in the supernatants of whole colon and duodenum tissue explants. Using an antibody array panel we detected increased secretion of inflammatory cytokines in the supernatant of the colon and the duodenum of *Muc2*$^{-/-}$ mice compared to wt counterparts, as shown in Fig 3C. The *Muc2*$^{-/-}$ duodenum was characterized by a robust response as illustrated by increased levels of Mig/CXCL9, MCP1, IL1α and IL1ra, in addition to C5a and IL16, the latter also induced in the colon, albeit at lower levels. IL23, instead, was uniquely expressed in the *Muc2*$^{-/-}$ colon. Of note, Mig/CXCL9, an Ifn-γ responsive gene, was secreted by Muc2$^{-/-}$ duodenum that uniquely showed upregulation of *Ifn-γ* mRNA (Fig. 3B); further, both IL16 and IL23 have been specifically linked to Crohn’s disease (29,30). Thus, these data clearly demonstrate that a reactive intestinal mucosa is associated with Muc2 deficiency, reflecting a limited inflammatory response.

To confirm that the exacerbation of the tumor phenotype we observed in compound double mutant *Muc2/Apc* mice was due to an inflammatory stimulus provided by Muc2 deficiency, we investigated whether the pattern of gene expression of intestinal epithelial cells of compound double mutant *Muc2*$^{-/-}$;*Apc*$^{1638N/+}$ mice was similar to that of *Muc2*$^{-/-}$ animals by qRT-PCR analysis of a subset of genes that were modulated in the Muc2$^{-/-}$ flat mucosa (Fig. 3A–B). Supplementary Fig. 8 shows that all the genes we tested were similarly regulated in double mutant *Muc2*$^{-/-}$;*Apc* $^{1638N/+}$ epithelial cells as in *Muc2*$^{-/-}$ mice. These data indicate that Muc2 deficiency in the *Apc* $^{1638N/+}$ background also results in a low grade inflammation reflected by the gene expression profile and that this most likely contributes to the more severe tumor phenotype in double mutant mice.

Discussion

We reported that genetic inactivation of the *Muc2* gene causes spontaneous development of tumors along the entire gastrointestinal tract without deregulating Wnt signaling. However, complex interaction between *APC*, a component of Wnt signaling fundamental to colon cancer initiation, and the *MUC2* gene is documented not only by data showing a reduction of goblet cells, and the mucins they produce, in tumors, but that reduced representation of goblet cells characterizes a subset of ACF, called mucin depleted foci (MDF) that are precancerous lesions (10). Thus, to further dissect interactions between MUC2 deficiency and alterated Wnt signaling, and to elucidate mechanisms of tumor formation in *Muc2*$^{-/-}$ mice, we crossed the *Muc2*$^{-/-}$ mouse with 2 mouse Apc initiated models of colon cancer, *Apc*$^{1638N/+}$ and *Apc*$^{Min/+}$. We observed an exacerbated tumor phenotype, shown by accelerated kinetics and increased tumor frequency in compound double mutant mice in which the *Muc2* mutation was present with either the *Apc*^{1638} or *Apc*^{Min} allele. Most impressive, in compound *Muc2/Apc* mutant mice there was a shift in tumor location towards the colon, which was particularly severe in *Muc2*$^{-/-}$;*Apc*$^{Min/+}$mice, characterized by a high density of tumors in the distal colon. The fewer proximal colon tumors support the hypothesis that the mouse distal colon is more permissive than the proximal for tumor formation (15,31). Tumor frequency in the colon was strongly dependent on *Muc2* gene dosage both in compound double mutant *Muc2*$^{+/-}$; *Apc*$^{1638N/+}$ and *Muc2*$^{+/-}$; *Apc*$^{Min/+}$ (Table 1A,B).

Molecular analysis of tumors from mice of different genotypes demonstrated that, contrary to tumors in *Muc2*$^{-/-}$ mice, Wnt signaling was altered in tumors of double mutant mice similarly to mutant *Apc* alone, reflected by nuclear accumulation of β-catenin, a hallmark of activated Wnt signaling, and increased levels of active, non-phosphorylated β-catenin. These data strongly suggest that deregulation of the Wnt pathway is the dominant mechanism of tumor formation in compound double mutant *Muc2/Apc* mice. However, it would be expected that the mechanism of tumor development, irrespective of initiating insult, would converge on obligatory steps. In fact, we previously demonstrated that c-Myc was elevated in Muc2$^{-/-}$ tumors as it is in mutant *Apc* initiated tumors (3), and here showed that Cox2 levels were induced in all tumors and that this expression was confined to the stromal compartment of the tumors. Thus, both c-Myc and Cox2 elevation appear to be obligatory steps for tumor formation regardless of etiology or differences in early events.

In tumors of *Apc*$^{1638N/+}$ mice, the wt *Apc* allele is most frequently inactivated by LOH (21). Increased frequency of inactivation by mutation, however, is detected in tumors of *Apc*$^{1638N/+}$ mice also deficient in components of the mismatch repair system (16). Interestingly we found that the molecular mechanism of inactivation of the wt *Apc* allele in tumors of compound double mutant mice is linked to *Muc2* gene dosage. Half of the *Muc2*$^{+/-}$;*Apc*$^{1638N/+}$ tumors exhibited truncating mutations in the wt *Apc* allele, the majority being point mutations, 50% of which were C to T transitions, the remaining being single nucleotide insertions or deletions. Increased point mutations, and an enrichment of C to T transitions, have been described in *Msh6*$^{-/-}$ mice that are deficient in mismatch repair. However, our studies in *Muc2*$^{-/-}$ and *Muc2/Apc*$^{1638N/+}$ tumors showed that, regardless of mutational status of the *Apc* allele, tumors did not exhibit instability at the homopolymeric or microsatellite loci assayed. Therefore, our data strongly suggest that MSI is not an early event in tumor formation in these mice.

Tumors that did not have *Apc* mutations exhibited LOH, and these 2 mechanisms were usually mutually exclusive, with the exception of 3 tumors that showed both mutational inactivation and LOH. These 3 samples may have contained more than 1 tumor, or may have been polyclonal (32).

In contrast, when the *Muc2* mutation was homozygous in *Muc2*$^{-/-}$;*Apc*$^{1638N/+}$ mice, there was considerable reduction of tumors with mutational inactivation of *Apc* compared to *Muc2*$^{+/-}$;*Apc*$^{1638N/+}$ tumors, yet surprisingly 72% (13/18) of tumors that were *Apc* mutation negative were also LOH negative. However, these *Muc2*$^{-/-}$;*Apc*^{1638N} tumors exhibited deregulated Wnt signaling, suggesting that activation of β-catenin occurred either through inactivation of *Apc* by mutation at other sites in the gene, by epigenetic mechanisms, or through alterations at another locus. As regards the latter, an obvious candidate, as a direct target, is β-catenin itself, observed in human tumors, albeit infrequently, to be mutated at potential phosphorylation sites through which Gsk3-β kinase targets β-catenin for degradation (33). However, we did not detect β-catenin mutations in DNA from tumors negative for both truncating mutation of *Apc* and LOH, at hot spots in exon 3 identified in rodent intestinal tumors induced by AOM (34). There are, however, additional mechanisms that result in β-catenin stabilization, (35,36), and the extent to which they play a role in these mice remains under investigation.

A wealth of experimental evidence has established the importance of inflammation in cancer initiation and progression (37,38), a phenotype that might be expected in the *Muc2*$^{-/-}$ mice with a compromised mucous barrier. Indeed, *Muc2*$^{-/-}$ mice displayed enhanced mucosal permeability (a four fold increase compared to wt mice -data not shown), a defect that has been detected preceding and predicting relapse in IBD patients and prior the onset of chronic immune-mediated histopathology in some mouse models of IBD (39,40). Furthermore, although the *Muc2*$^{-/-}$ mouse on a C57BL/6 background exhibited no obvious intestinal inflammation in the barrier facility where our mice are housed, we recently reported that *Muc2* deficient mice, on a congenic 129SV background, housed elsewhere, spontaneously developed early colitis that aggravates with age (41). We therefore hypothesize that *Muc2* deficiency causes a low grade inflammation important in tumorigenesis and in exacerbating tumor formation initiated by *Apc* mutation. Moreover, the substantial increase in colonic tumor burden in compound double mutant *Muc2/Apc* mice is reminiscent of increased colon tumor phenotype reported for *Apc*$^{Min/+}$ mice treated with dextran sodium sulfate (DSS) that induces intestinal inflammation, and in compound *Smad3*$^{-/-}$*Apc*^{Min} mice in which inactivation of *Smad3* triggers an inflammatory response (15). Consistent with this, we identified a gene expression pattern in the flat mucosa of *Muc2*$^{-/-}$ mice characteristic of low level inflammation. Most important, one third of the gene expression changes in the duodenum of *Muc2*$^{-/-}$ mice that are associated with inflammation are similarly changed in the colon, further supporting our hypothesis that lack of Muc2 generates low levels of inflammation. Changes included decreased expression of detoxifying phase I and II genes involved in drug biotransformation and elimination. The importance of these defense mechanisms in probability of tumor formation is underscored by the fact that many of these intestinal detoxification and glutathione biosynthetic enzymes are induced by phytochemicals as well as chemoprotective pharmacological agents, and further, that natural dietary compounds that induce phase I and II detoxifying genes as well as antioxidant genes in the flat mucosa, decrease tumor formation in *Apc*$^{Min/+}$mice (42). Thus, reduced levels in the normal intestinal tract of *Muc2*$^{-/-}$ mice likely contribute to tumorigenesis by compromising the ability of intestinal cells to mount an effective response to endogenous and exogenous stresses.

In contrast, glutathione peroxidase 2 (*Gpx2*, an intestine specific selenoprotein), and glutathione reductase, were robustly upregulated in the epithelium of *Muc2*$^{-/-}$ mice. These enzymes are induced during the antioxidant response (43). Thus, their upregulation in the

NIH-PA Author Manuscript

NIH-PA Author Manuscript

Muc2 mutant mouse suggests that the normal appearing mucosa in these mice is indeed under oxidative stress. Collectively, these data suggest that in the flat mucosa of *Muc2*$^{-/-}$ mice there are perturbations in the detoxifying/antioxidant response resulting in increased exposure of epithelial cells to genotoxic insult that contributes to tumorigenesis.

The mucus barrier is the first line of defense that physically separates underlying epithelial cells and the intestinal microbiota, establishing a link between mucins, innate immunity and inflammatory response (44). In agreement, in Muc2 deficient mice we detected induction of genes of the innate immune system, the majority of which are expressed by Paneth cells (45), including upregulation of secretory phospholipase group IIA and V, *Pla2g2a* and *Pla2g5* that share antibacteriocidal properties. Interestingly, the *Pla2g2a* gene, mutated in C57BL/6 mice, is a modifier of the *Apc*^{Min} phenotype and is also a modifier of the *Muc2*$^{-/-}$ tumor phenotype, as a functional *Pla2g2a* allele confers resistance to tumor development to *Muc2*$^{-/-}$ mice (Fijneman *et al*., Cancer Science, in press), further supporting the hypothesis that impaired mucosal protection increases risk of tumor development. Moreover, these results indicate that stress to the mucosa may, at least in part, stem from increased exposure to microbial populations that occupy the intestinal lumen. In this regard, we documented a robust increase of several members of the C-type lectin family in *Muc2*$^{-/-}$ mice, genes with well established bacteriocidal effects (46), and elevation of *Ccl6* and *Ccl28*, members of the CC chemokine family expressed by epithelial cells that promote antimicrobial immunity. Interestingly, despite the increased expression of antibacterial polypeptides and the increased mucosal permeability, we did not detect bacterial translocation to mesenteric lymph nodes (S. Guilmeau & A. Velcich, unpublished), in agreement with the absence of histopathological manifestations.

The role of mucins in the cross-talk that determines the inflammatory response is further emphasized by our data demonstrating increased release of inflammatory cytokines in ex vivo explants of whole colon and duodenum of *Muc2*$^{-/-}$ compared to wt mice. Intriguingly, IL23, shown to be linked to Crohn's disease by inducing a T helper type 17 pro-inflammatory response (47,48), was significantly enhanced in the colon of *Muc2*$^{-/-}$ mice, possibly explaining the aggravated colonic phenotype of compound double mutant *Muc2/Apc* mice. Furthermore, our data showing the concomitant induction of IL1α and its receptor antagonist IL1ra suggest that the intestinal tract has complex regulatory mechanisms that maintain immune homeostasis and that the level of inflammation is linked to the extent to which the balance between inflammatory stimuli and the host compensatory response is subverted.

In conclusion, we emphasize that the *Muc2* mutant mouse model, alone and in combination with the *Apc* mutation, has unique physiopathological features useful for dissecting complex relationships among tumor development, environmental stresses on the mucosa, and chronic inflammation. In relation to the development of human colon cancer, we have noted the depletion of globlet cells, and the mucins they produce, in ACF, and therefore that this can contribute to focal development and progression of disease. Interestingly, we found that *Muc2* haploinsufficiency may impart a modest increased risk of tumor development, as illustrated by the detection of one tumor in the small intestine of a single 52 week old mouse, a risk that becomes greatly exacerbated in the mutant *Apc* background. This is important because it suggests that variations in *MUC2* could modulate tumor development by affecting the landscape of the intestinal tract. In this regard, it was reported that polymorphisms in the number of tandem repeat region (VNTR) of the *MUC2* gene (49), that have the potential to contribute to modulating the protective barrier established by mucins, were not linked to susceptibility to inflammation (50). In contrast, our data suggest that variation of MUC2 amount may contribute to the risk for colon cancer development.

NIH-PA Author Manuscript
NIH-PA Author Manuscript

Supplementary Material

Refer to Web version on PubMed Central for supplementary material.

Acknowledgments

We thank D. Reynolds for help in the generation and interpretation of the microsatellite instability data, and S. Nasser for histopathology, and M. Lesser and E. Livote for statistical analysis.

This study was supported by the National Institute of Health grants DK058245; U54CA100926; and Cancer Center Grant P30-13330 and a grant from the University of Minnesota Academic Health Center to R.T.C..

References

1. Hollingsworth MA, Swanson BJ. Mucins in cancer: protection and control of the cell surface. Nat Rev Cancer 2004;4:45–60. [PubMed: 14681689]
2. Andrianifahanana MMN, Batra SK. Regulation of mucin expression: Mechanistic aspects and implications for cancer and inflammatory diseases. Bioch Bioph Acta 2006;1765:189–222.
3. Velcich A, Yang W, Heyer J, et al. Colorectal cancer in mice genetically deficient in the mucin Muc2. Science 2002;295:1726–1729. [PubMed: 11872843]
4. Nishisho I, Nakamura Y, Miyoshi Y, et al. Mutations of chromosome 5q21 genes in FAP and colorectal cancer patients. Science 1991;253:665–669. [PubMed: 1651563]
5. Groden J, Thliveris A, Samowitz W, et al. Identification and characterization of the familial adenomatous polyposis coli gene. Cell 1991;66:589–600. [PubMed: 1651174]
6. Kinzler KW, Nilbert MC, Su LK, et al. Identification of FAP locus genes from chromosome 5q21. Science 1991;253:661–665. [PubMed: 1651562]
7. Sancho E, Batlle E, Clevers H. Signaling pathways in intestinal development and cancer. Annu Rev Cell Dev Biol 2004;20:695–723. [PubMed: 15473857]
8. Leow CC, Romero MS, Ross S, Polakis P, Gao WQ. Hath1, Down-Regulated in Colon Adenocarcinomas, Inhibits Proliferation and Tumorigenesis of Colon. Cancer Cells Cancer Res 2004;64:6050–6057.
9. Blache P, van de Wetering M, Duluc I, et al. SOX9 is an intestine crypt transcription factor, is regulated by the Wnt pathway, and represses the CDX2 and MUC2 genes. J Cell Biol 2004;166:37–47. [PubMed: 15240568]
10. Caderni G, Femia AP, Giannini A, et al. Identification of Mucin-depleted Foci in the Unsectioned Colon of Azoxymethane-treated Rats: Correlation with Carcinogenesis. Cancer Res 2003;63:2388–2392. [PubMed: 12750256]
11. Pretlow TP, Pretlow TG. Mutant KRAS in aberrant crypt foci (ACF): initiation of colorectal cancer? Biochim Biophys Acta 2005;1756:83–96. [PubMed: 16219426]
12. Fodde R, Edelman W, Yang K, et al. A targeted chain-termination mutation in the mouse *Apc* gene results in multiple intestinal tumors. Proc Natl Acad Sci USA 1994;91:8969–8973. [PubMed: 8090754]
13. Su LK, Kinzler KW, Vogelstein B, et al. Multiple intestinal neoplasia caused by a mutation in the murine homolog of the APC gene. Science 1992;256:668–670. [PubMed: 1350108]
14. Takuji Tanaka HK, Rikako Suzuki, Kazuya Hata, Shigeyuki Sugie, Naoko Niho, Katsuhisa Sakano, Mami Takahashi, Keiji Wakabayashi. Dextran sodium sulfate strongly promotes colorectal carcinogenesis in ApcMin/+ mice: Inflammatory stimuli by dextran sodium sulfate results in development of multiple colonic neoplasms. Int J Cancer 2006;118:25–34. [PubMed: 16049979]
15. Sodir NM, Chen X, Park R, et al. Smad3 Deficiency Promotes Tumorigenesis in the Distal Colon of ApcMin/+ Mice. Cancer Res 2006;66:8430–8438. [PubMed: 16951153]
16. Kuraguchi M, Yang K, Wong E, et al. The distinct spectra of tumor-associated Apc mutations in mismatch repair-deficient Apc1638N mice define the roles of MSH3 and MSH6 in DNA repair and intestinal tumorigenesis. Cancer Res 2001;61:7934–7942. [PubMed: 11691815]

17. Guda K, Upender MB, Belinsky G, et al. Carcinogen-induced colon tumors in mice are chromosomally stable and are characterized by low-level microsatellite instability. Oncogene 2004;23:3813–3821. [PubMed: 15021908]
18. Oshima M, Dinchuk JE, Kargman SL, et al. Suppression of Intestinal Polyposis in Apc[Delta]716 Knockout Mice by Inhibition of Cyclooxygenase 2 (COX-2). Cell 1996;87:803–809. [PubMed: 8945508]
19. Shattuck-Brandt RL, Varilek GW, Radhika A, Yang F, Washington MK, DuBois RN. Cyclooxygenase 2 expression is increased in the stroma of colon carcinomas from IL-10−/− mice. Gastroenterology 2000;118:337–345. [PubMed: 10648462]
20. Hull MA, Scott ATN, Bonifer C, Coletta PL. Cyclooxygenase 2 is up-regulated and localized to macrophages in the intestine of Min mice. Br J Cancer 1999;79:1399–1405. [PubMed: 10188882]
21. Smits R, Kartheuser A, Jagmohan-Changur S, et al. Loss of Apc and the entire chromosome 18 but absence of mutations at the Ras and Tp53 genes in intestinal tumors from Apc1638N, a mouse model for Apc-driven carcinogenesis. Carcinogenesis 1997;18:321–327. [PubMed: 9054624]
22. Aitken AE, Richardson TA, Morgan ET. Regulation of drug-metabolizing enzymes and transporters in inflammation. Annu Rev Pharmacol Toxicol 2006;46:123–149. [PubMed: 16402901]
23. Masubuchi Y, Horie T. Endotoxin-mediated disturbance of hepatic cytochrome P450 function and development of endotoxin tolerance in the rat model of dextran sulfate sodium-induced experimental colitis. Drug Metab Dispos 2004;32:437–441. [PubMed: 15039297]
24. Cash HL, Witham CBCL, Hooper LV. Symbiotic bacteria direct expression of an intestinal bactericidal lectin. Science 2006;313:1126–1130. [PubMed: 16931762]
25. McVay LD, Keilbaugh SA, Wong TMH, et al. Absence of bacterially induced RELM{beta} reduces injury in the dextran sodium sulfate model of colitis. J Clin Invest 2006;116:2914–2923. [PubMed: 17024245]
26. Flo TH, Smith KD, Sato S, et al. Lipocalin 2 mediates an innate immune response to bacterial infection by sequestrating iron. Nature 2004;432:917–921. [PubMed: 15531878]
27. Hieshima K, Kawasaki Y, Hanamoto H, et al. CC Chemokine Ligands 25 and 28 Play Essential Roles in Intestinal Extravasation of IgA Antibody-Secreting Cells. J Immunol 2004;173:3668–3675. [PubMed: 15356112]
28. Coelho AL, Schaller MA, Benjamim CF, Orlofsky AZ, Hogaboam CM, Kunkel SL. The Chemokine CCL6 Promotes Innate Immunity via Immune Cell Activation and Recruitment. J Immunol 2007;179:5474–5482. [PubMed: 17911634]
29. Seegert D, Rosenstiel P, Pfahler H, Pfefferkorn P, Nikolaus S, Schreiber S. Increased expression of IL-16 in inflammatory bowel disease. Gut 2001;48:326–332. [PubMed: 11171821]
30. Hue S, Ahern P, Buonocore S, et al. Interleukin-23 drives innate and T cell-mediated intestinal inflammation. J Exp Med 2006;203:2473–2483. [PubMed: 17030949]
31. Hinoi T, Akyol A, Theisen BK, et al. Mouse Model of Colonic Adenoma-Carcinoma Progression Based on Somatic Apc Inactivation. Cancer Res 2007;67:9721–9730. [PubMed: 17942902]
32. Merritt AJ, Gould KA, Dove WF. Polyclonal structure of intestinal adenomas in ApcMin/+ mice with concomitant loss of Apc+ from all tumor lineages. Proc Natl Acad Sci U S A 1997;94:13927–13931. [PubMed: 9391129]
33. Polakis P. The oncogenic activation of [beta]-catenin. Current Opinion in Genetics & Development 1999;9:15–21. [PubMed: 10072352]
34. Kohno H, Suzuki R, Sugie S, Tanaka T. Catenin mutations in a mouse model of inflammation-related colon carcinogenesis induced by 1,2-dimethylhydrazine and dextran sodium sulfate. Cancer Science 2005;96:69–76. [PubMed: 15723650]
35. Haq S, Michael A, Andreucci M, et al. Stabilization of beta -catenin by a Wnt-independent mechanism regulates cardiomyocyte growth. Proceedings of the National Academy of Sciences 2003;100:4610–4615.
36. Tian Q, Feetham MC, Tao WA, et al. Proteomic analysis identifies that 14-3-3{zeta} interacts with {beta}-catenin and facilitates its activation by Akt. Proceedings of the National Academy of Sciences 2004;101:15370–15375.
37. Clevers H. At the crossroads of inflammation and cancer. Cell 2004;118:671–674. [PubMed: 15369667]

38. Chen R, Rabinovitch PS, Crispin DA, Emond MJ, Bronner MP, Brentnall TA. The initiation of colon cancer in a chronic inflammatory setting. Carcinogenesis 2005;26:1513–1519. [PubMed: 15860506]
39. Olson TS, Reuter BK, Scott KGE, et al. The primary defect in experimental ileitis originates from a nonhematopoietic source. J Exp Med 2006;203:541–552. [PubMed: 16505137]
40. Ahmad R, Raina D, Trivedi V, et al. MUC1 oncoprotein activates the I[kappa]B kinase [beta] complex and constitutive NF-[kappa]B signalling. Nat Cell Biol 2007;9:1419–1427. [PubMed: 18037881]
41. Van der Sluis M, De Koning BAE, De Bruijn ACJM, et al. Muc2-Deficient Mice Spontaneously Develop Colitis, Indicating That MUC2 Is Critical for Colonic Protection. Gastroenterology 2006;131:117–129. [PubMed: 16831596]
42. Shen G, Khor TO, Hu R, et al. Chemoprevention of Familial Adenomatous Polyposis by Natural Dietary Compounds Sulforaphane and Dibenzoylmethane Alone and in Combination in ApcMin/+ Mouse. Cancer Res 2007;67:9937–9944. [PubMed: 17942926]
43. Winyard PG, Moody CJ, Jacob C. Oxidative activation of antioxidant defence. Trends in Biochemical Sciences 2005;30:453–461. [PubMed: 15996871]
44. Linden SK, Sutton P, Karlsson NG, Korolik V, McGuckin MA. Mucins in the mucosal barrier to infection. Mucosal Immunol 2008;1:183–197. [PubMed: 19079178]
45. Salzman NH, Underwood MA, Bevins CL. Paneth cells, defensins, and the commensal microbiota: A hypothesis on intimate interplay at the intestinal mucosa. Seminars in Immunology 2007;19:70–83. [PubMed: 17485224]
46. Dann SME. Lars Innate immune defenses in the intestinal tract. Curr opin Gastroenterol 2007;23:115–120. [PubMed: 17268238]
47. David Yen JC, Heleen Scheerens, Frédérique Poulet, Terrill McClanahan, Brent Mckenzie, Melanie A Kleinschek, Alex Owyang, Jeanine Mattson, Wendy Blumenschein, Erin Murphy, Manjiri Sathe, Daniel J Cua, Robert A Kastelein, Donna Rennick. IL-23 is essential for T cell mediated colitis and promotes inflammation via IL-17 and IL-6. J Clin Invest 2006;116:1310–1316. [PubMed: 16670770]
48. Ishigame, YIaH. The IL-23/IL-17 axis in inflammation. J Clin Invest 2006;116:1218–1222. [PubMed: 16670765]
49. Toribara NWJRG Jr, Culhane PJ, Lagace RE, Hicks JW, Petersen GM, Kim YS. MUC-2 human small intestinal mucin gene structure. Repeated arrays and polymorphism. J Clin Invest 1991;88:1005–1013. [PubMed: 1885763]
50. Swallow DM, Vinall LE, Gum JR, et al. Ulcerative colitis is not associated with differences in MUC2 mucin allele length. J Med Genet 1999;36:859–860. [PubMed: 10636731]

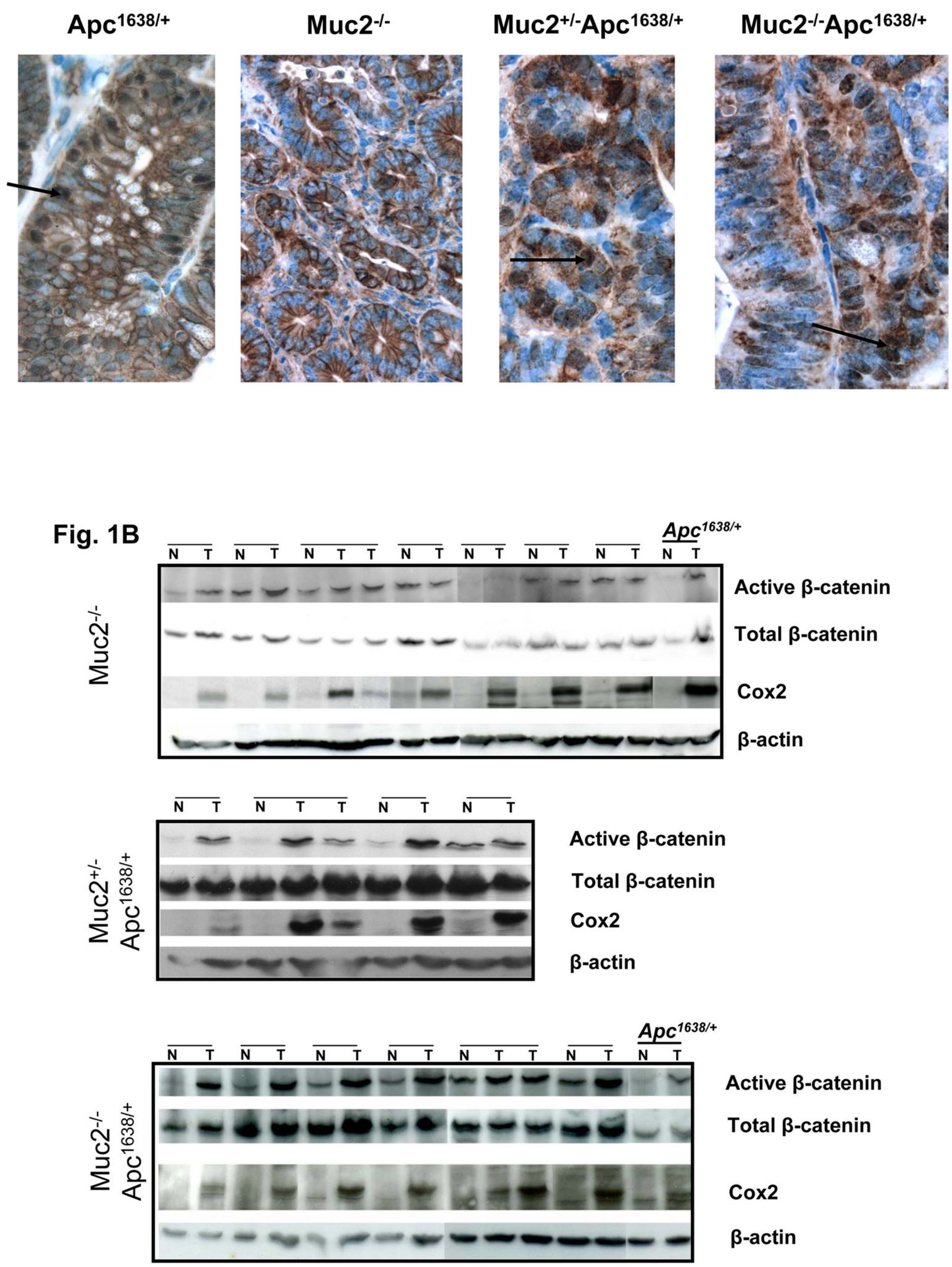

Fig. 1.

β-catenin expression in tumors of *Apc*$^{1638N/+}$, *Muc2*$^{-/-}$ and compound double mutant *Muc2*$^{-/-}$;*Apc*$^{1638N/+}$ mice. Panel A shows representative immunohistochemical analysis of β-catenin expression in tumors of mice of the indicated phenotype. β-catenin nuclear localization is observed in *Apc*$^{1638N/+}$and double mutant *Muc2/Apc*$^{1638N/+}$ tumors (arrows), but it is not detected in *Muc2*$^{-/-}$ tumors. Total number of tumors analyzed were 3 for *Apc*$^{1638N/+}$ and 6 for each *Muc2*$^{-/-}$ and double mutant *Muc2*$^{+/-}$; *Muc2*$^{-/-}$;*Apc*$^{1638N/+}$ tumors. Panel B shows the levels of expression of activated (non-phosphorylated) and total β-catenin as well as Cox2 in cell extracts of paired normal and tumor of the indicated genotypes. β-actin levels were determined as controls for equal loading and gel transfer.

NIH-PA Author Manuscript
NIH-PA Author Manuscript

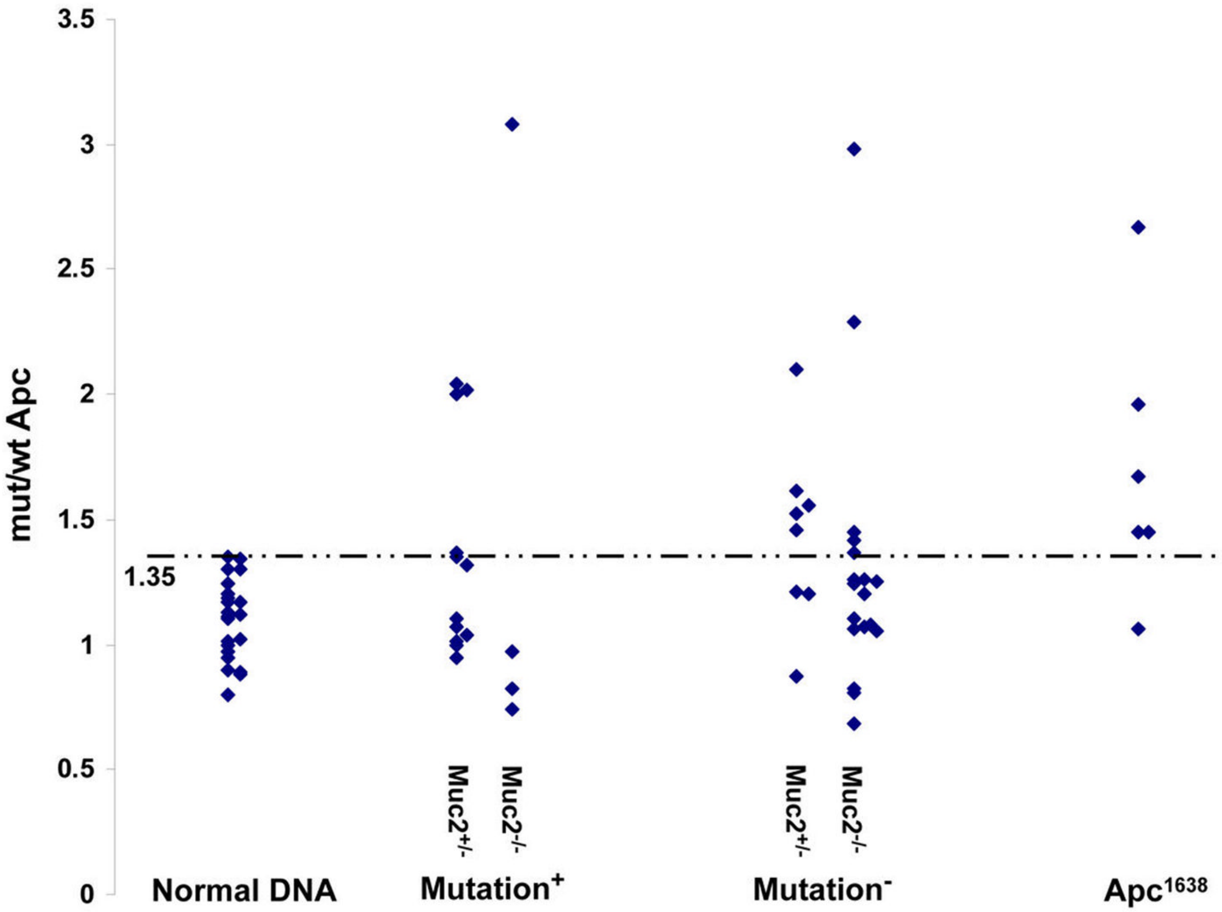

Fig. 2.

Analysis of loss of heterozygosity of the wt *Apc* allele in tumors of compound double mutant *Muc2*$^{+/-}$;*Apc*$^{1638N/+}$ and *Muc2*$^{-/-}$;*Apc*$^{1638N/+}$ mice. Quantitative genomic PCR assay was used to determine the ratio of mutant and wt *Apc* alleles in controls and tumor DNAs, as described in Materials and Methods. LOH was defined when the value of the ratio of mut/wt allele in tumor DNA was greater than 1.35, the highest value of mut/wt ratio in the control normal DNA samples (dotted line). Normal DNA was isolated from normal mucosa and tails of double mutant *Muc2/Apc*$^{1638N/+}$ mice as well as normal mucosa, liver and tail of *Apc*$^{1638N/+}$ mice. Mutation positive and negative indicates set of tumor DNAs that were positive or negative for mutation inactivation of the wt *Apc* allele by the IVTT assay, respectively. *Apc*$^{1638N/+}$ indicates DNAs isolated from *Apc*$^{1638N/+}$ tumors.

NIH-PA Author Manuscript
NIH-PA Author Manuscript

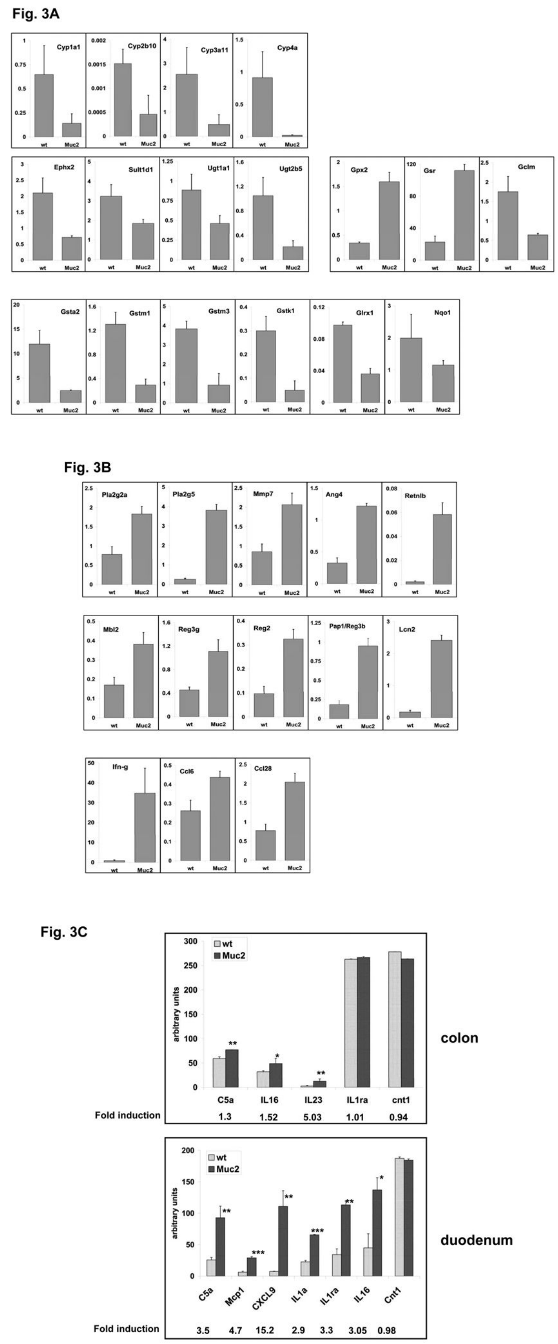

Fig. 3.

qRT-PCR validation of microarray results for a selected number of genes. cDNA was generated from total RNA independently prepared from small intestine epithelial cells isolated from three 3 month old *Muc2*$^{-/-}$ mice and 3 age, and gender matched wt littermates and used in qPCR reactions, as described in Materials and Methods. Candidate genes mRNA levels are expressed relative to the value of β-actin or Rpl41 (ribosomal protein 41). Panel A shows changes in expression in Muc2$^{-/-}$ normal epithelial cells compared to wt samples for detoxifying class I and II as well as antioxidant genes. B. Relative expression levels of genes involved in innate immune response and inflammation. C. Antibody array analysis of supernatants of colonic (top panel) and duodenal (bottom panel) ex-vivo explants (3 mice/genotype) after 24 hours cultivation in serum-free medium at 37 °C. Densitometric scanning of array film images were performed and signal intensities for the indicated cytokines/chemokines were determined using ImageQuant Software (Molecular Dynamics) and expressed in arbitrary units (mean ± standard error) upon normalization to tissue weight.

$^{*}P < 0.05$; $^{**}P < 0.005$; $^{***}P < 0.0001$ by paired *t* test.

Table 1

Table 1A. Tumor multiplicity in *Muc2* mutant, *Apc*$^{1638N/+}$, and compound double mutant mice

Genotype months	GI tract	*Apc*$^{1638N/+}$	*Muc2*$^{+/-}$	*Muc2*$^{-/-}$	*Muc2*$^{+/-}$*Apc*$^{1638N/+}$	*Muc2*$^{-/-}$*Apc*$^{1638N/+}$
3	SI	0.69 ± 0.1	0	0.33 ± 0.16	0.95 ±0.21[1]	1.73 ± 0.55[2]
	LI	0	0	0.06 ± 0.06	0	0.55 ± 0.22[a]
6	SI	1.47 ± 0.33	0	1.36 ± 0.45	1.81 ± 0.37[1]	5.16 ±.098[2,b]
	LI	0.06 ± 0.06	0	0.09 ± 0.09	0.24 ± 0.15	2.24 ± 0.54[1,a]
12	SI	2.91 ± 0.5	0.18 ± 0.18	1.07 ± 0.53	4.91 ± 1.09[1]	5.5 ± 0.69[1,b]
	LI	0.18 ± 0.18	0	0.39 ± 0.18	0.46 ± 0.21[3,b]	3.92 ± 1.06[2,a]

Table 1B. Tumor multiplicity and incidence in double mutant compound *Muc2/Apc*$^{Min/+}$ mice at 75 days of age

	Genotype	*Muc2*$^{+/+}$*Apc*$^{Min/+}$	*Muc2*$^{+/-}$*Apc*$^{Min/+}$	*Muc2*$^{-/-}$*Apc*$^{Min/+}$
	No mice	20	25	14
	SI tumor multiplicity	58.5 ± 44	90 ± 40	141 ± 99 [b,2]
LI	Tumor multiplicity	0.15 ± 0.5	1.2 ± 1.3 [c]	38 ± 11.2 [a,1]
	incidence	30%	68%	100%

SI = Small Intestine; LI = Large Intestine; Data are expressed as Mean ± SEM. Mann-Whitney test:

[1] $P < 0.001$;

[2] $P < 0.01$;

[3] $P < 0.05$ compared to *Muc2*$^{-/-}$ mice

[a] $P < 0.001$;

[b] $P < 0.01$;

[c] $P < 0.05$ compared to *Apc*$^{1638N/+}$ mice

SI = Small Intestine; LI = Large Intestine

NIH-PA Author Manuscript
NIH-PA Author Manuscript

Wilcoxon Rank Sum test:

[1] $P = 1.3\times10^{-10}$;

[2] $P = 0.02$; compared to *Muc2*$^{+/-}$ *Apc*$^{Min/+}$ mice

[a] $P \ll 1\times10^{-10}$;

[b] $P < 0.001$;

[c] $P < 0.05$ compared to *Apc*$^{Min/+}$ mice

NIH-PA Author Manuscript
NIH-PA Author Manuscript

Table 2

Analysis of truncation mutation in intestinal tumors of compound double mutant *Muc2*/*Apc*$^{1638N/+}$ mice

Genotype	*Muc2*$^{-/-}$	*Muc2*$^{+/-}$*Apc*$^{1638N/+}$	*Muc2*$^{-/-}$*Apc*$^{1638N/+}$	*Apc*$^{1638N/+}$ *	*Mlh1*$^{-/-}$*Apc*$^{1638N/+}$*
Number tumors Analyzed	30	24	27		
Frequency Apc mutations	0	12 (50%)	4 (14.8%)	< 30%	65%
Base substitutions		8/12	4/4		
Frame-shift		4/12	0		

* data from Kuragachi et al.(19)

Table 3

Analysis of inactivation of the wt *Apc* allele as a function of *Muc2* gene dosage

	Mutation − LOH +	**Mutation + LOH −**	**Mutation+ LOH +**	**Mutation − LOH −**
LOH	10		5	
Muc2$^{+/-}$*Apc*$^{1638N/+}$ (n =20)	5	8	4	3
Muc2$^{-/-}$*Apc*$^{1638N/+}$ (n = 22)	5	3	1	13

n = number of tumors analyzed